







## V. CONCLUSIONS

The experimental results confirm the validity of the concept and the dimensional values obtained by simulation.

Among the advantages, worth to mention that this antenna has the input characteristic impedance of  $50\Omega$ , being easy to feed with usual coaxial cables through a common mode choke balun (**balanced-unbalanced**). The radiation pattern is omnidirectional and has axial circular polarization, obtained by design without an additional phase shifting circuit. It has a simple mechanical structure with only few electrical contacts and makes use of a single central antenna mast (e.g. UV resistant PVC pipe) that houses the coaxial cable, the choke balun and protects the connectors from the elements.

This antenna can be used as well for the radio meteor detection receiving stations, provided that the gain is high enough to cover the required link budget.

Outdoor impedance and SWR measurements, as well as radiation pattern measurements of the test antenna, using LEO (Low Earth Orbit) artificial satellites as reference radiofrequency sources, are in view. A full scale antenna prototype is intended to be used, in a first step, for meteor scatter and Es (Sporadic E) communications in the 50MHz frequency band.

## REFERENCES

- [1] A. Martínez Picar, S. Ranvier, M. Anciaux and H. Lamy, "Modeling and calibration of BRAMS antenna systems," Proceedings of the International Meteor Conference, Giron, France, pp. 201-206, September 2014.
- [2] A. Martínez Picar, C. Marque, M. Anciaux and H. Lamy, "Directional pattern measurement of the BRAMS beacon antenna system," Proceedings of the International Meteor Conference, Mistelbach, Austria, pp. 177-179, August 2015.
- [3] C. Steyaert, "The VVS meteor beacon," Proceedings of the International Meteor Conference, Oostmalle, Belgium, pp. 25-33, September 2005.
- [4] M.-Y. Yamamoto, H. Horiuchi, G. Okamoto, H. Hamaguchi and K. Noguchi, "Development of HRO interferometer at Kochi University of Technology," Proceedings of the International Meteor Conference, Roden, The Netherlands, pp. 117-125, September 2006.
- [5] W. K. Hocking, B. Fuller and B. Vandeppeer, "Real-time determination of meteor related parameters utilizing modern digital technology," The Journal of Atmospheric and Solar-Terrestrial Physics, vol. 63, pp. 155-169, 2001.
- [6] S. N. Nathwani and D. H. Trivedi, "Design of cross dipole antenna for the GPS band," ResearchGate GmbH, March 2019.
- [7] M. Matsunaga, "A circularly polarized spiral/loop antenna and its simple feeding mechanism," Modern Antenna Systems, M. A. Matin, IntechOpen, 2017.
- [8] B. Rama Rao, W. Kunysz, R. Fante and K. McDonald, "GPS/GNSS antennas," Artech House, 2013.
- [9] I. Radnovic, A. Nestic and B. Milovanovic, "A new type of turnstile antenna," IEEE Antennas and Propagation Magazine, Vol. 52, No.5, October 2010.
- [10] \*\*\*, "The European table of frequency allocations and applications," European Conference of Postal and Telecommunications Administrations, March 2019.
- [11] M. Mori, MMANA-GAL antenna analyzer software, <http://hamsoft.ca>.
- [12] C. E. Lesanu, A. Done, A. M. Cailan and A. Graur, "Vertical polarized antennas for Low-VHF radio meteor detection," International Conference on Development and Application Systems, Suceava, Romania, May 2018.

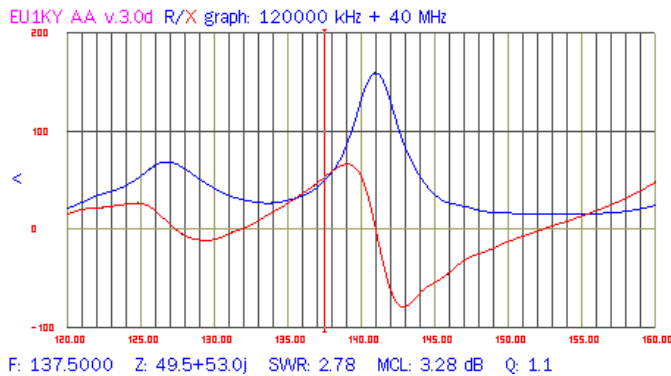


Fig. 8. The impedance components R,X measured for the inductive (long) dipole.

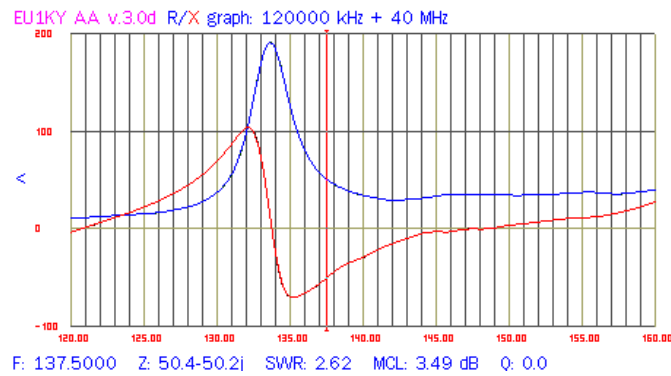


Fig. 9. The impedance components R,X measured for the capacitive (short) dipole.

After fitting the two dipoles in parallel, the total impedance of the obtained radiant system was measured (Fig. 10), on the 137.5MHz central frequency of interest, its value being  $Z=53.5-j0.6$ . The standing wave ratio measured on the central frequency is  $SWR=1.07$ . The bandwidth obtained for a standing wave ratio of 1:1.5 is  $\sim 26\text{MHz}$  (128.4-154.6MHz).

These impedance measurements were performed indoors, in an enclosure not treated in terms of the radio frequency field, with dimensions in all directions of about  $3\lambda$ , the presence of adjacent structures presumably influencing the obtained results.

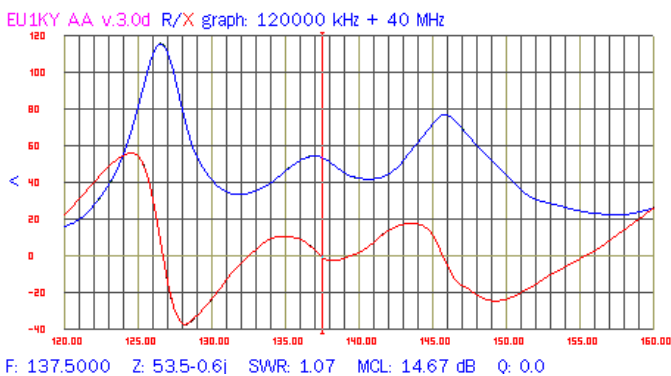


Fig. 10. The complex conjugate antenna measured impedance components R,X.